

ACCURACY OF MAGNETIC RESONANCE BASED SUSCEPTIBILITY MEASUREMENTS

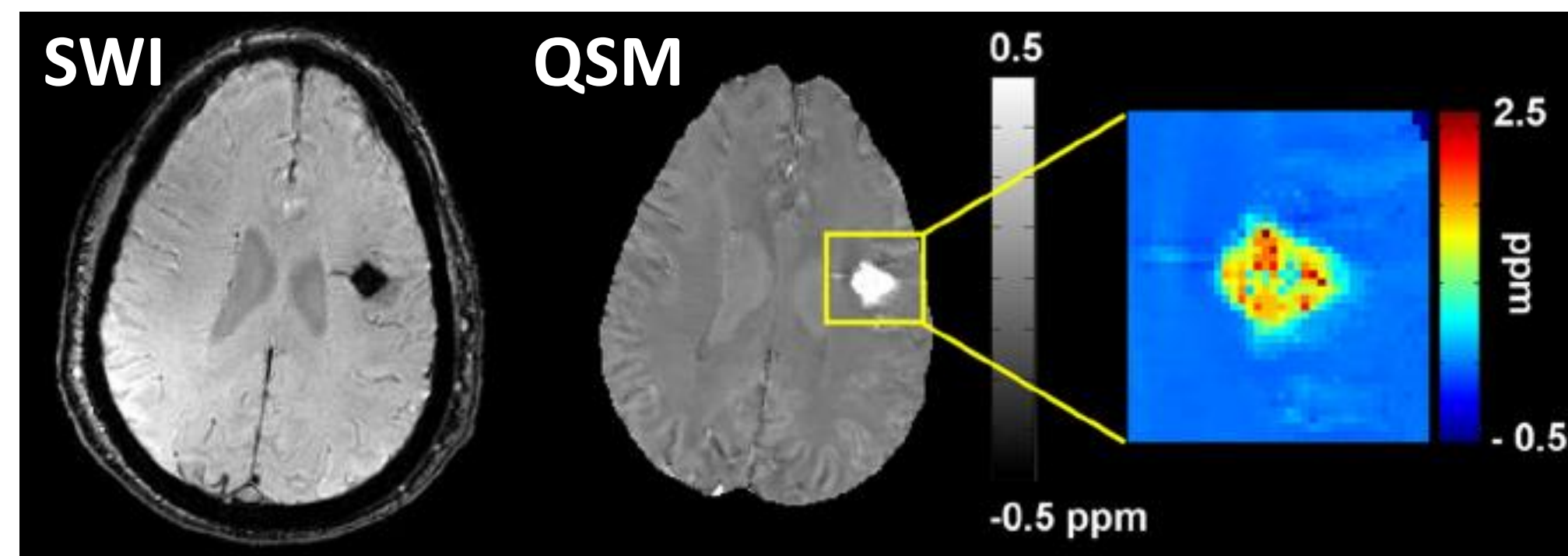
Hannah Erdevig¹, Slavka Carnicka², Katy Keenan², Karl Stupic², Stephen Russek²

¹University of Colorado, Boulder, ²National Institute of Standards and Technology, Boulder

SUSCEPTIBILITY MEASUREMENTS IN MEDICINE

Quantitative Susceptibility Mapping (QSM) is increasingly being used to map neurological diseases, blood oxygen content and iron overload in the heart and liver. NIST is working with RSNA and ISMRM to develop an SI-traceable susceptibility phantom as a common reference standard for QSM. Here, we assess the accuracy of the standard models used to extract magnetic susceptibility measurements from MRI.

How accurately can we measure susceptibility in vivo?



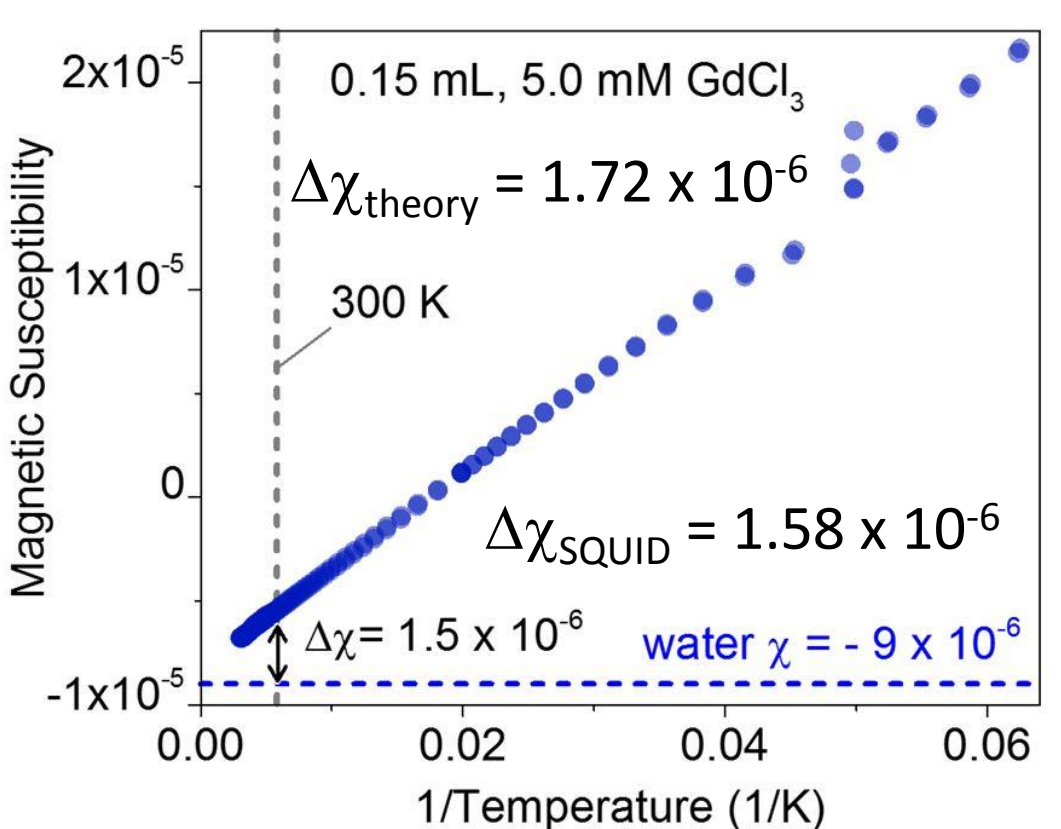
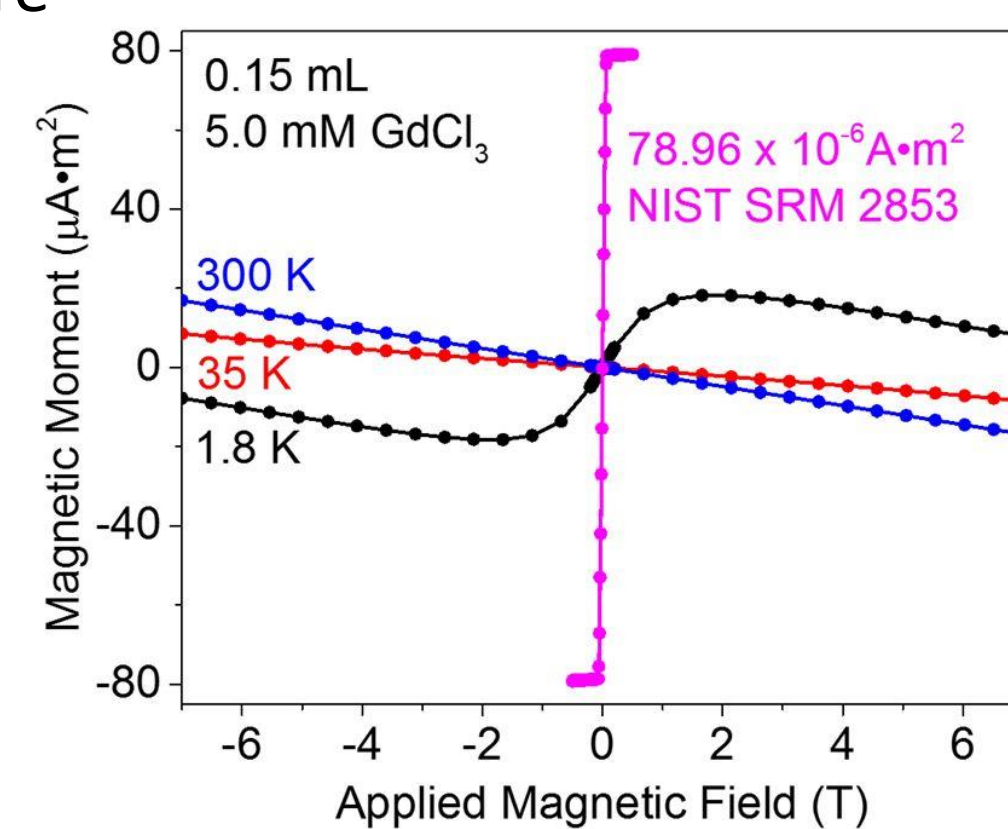
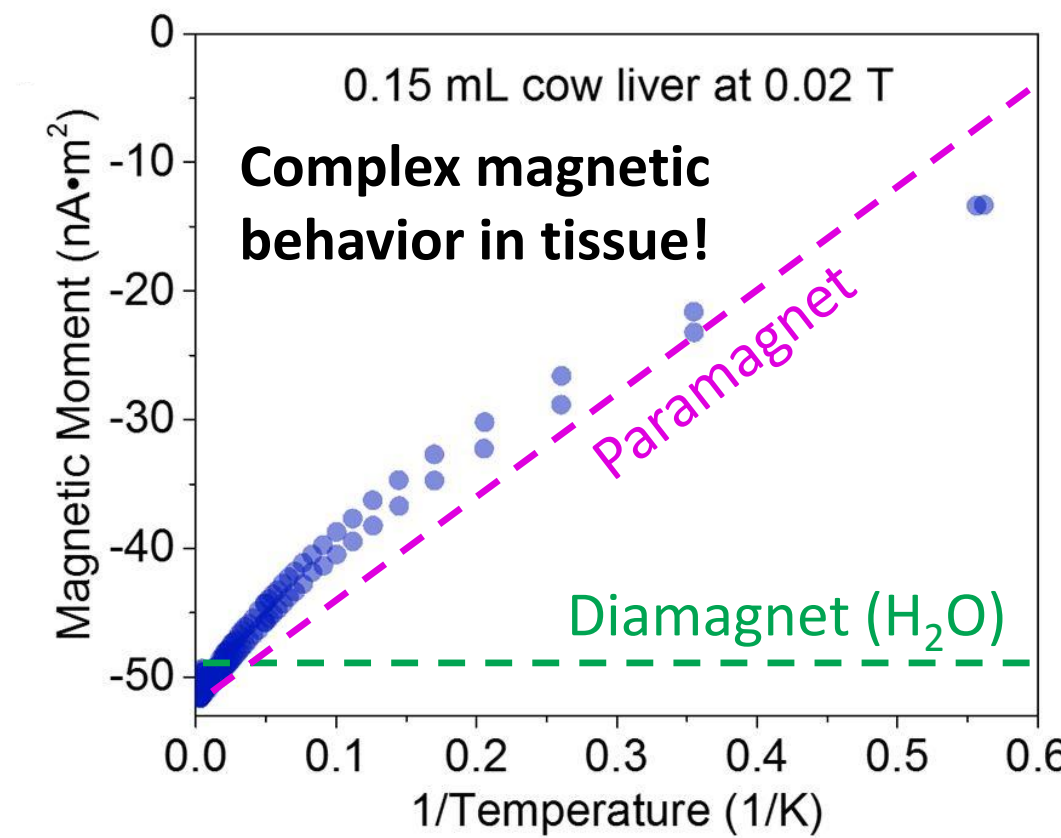
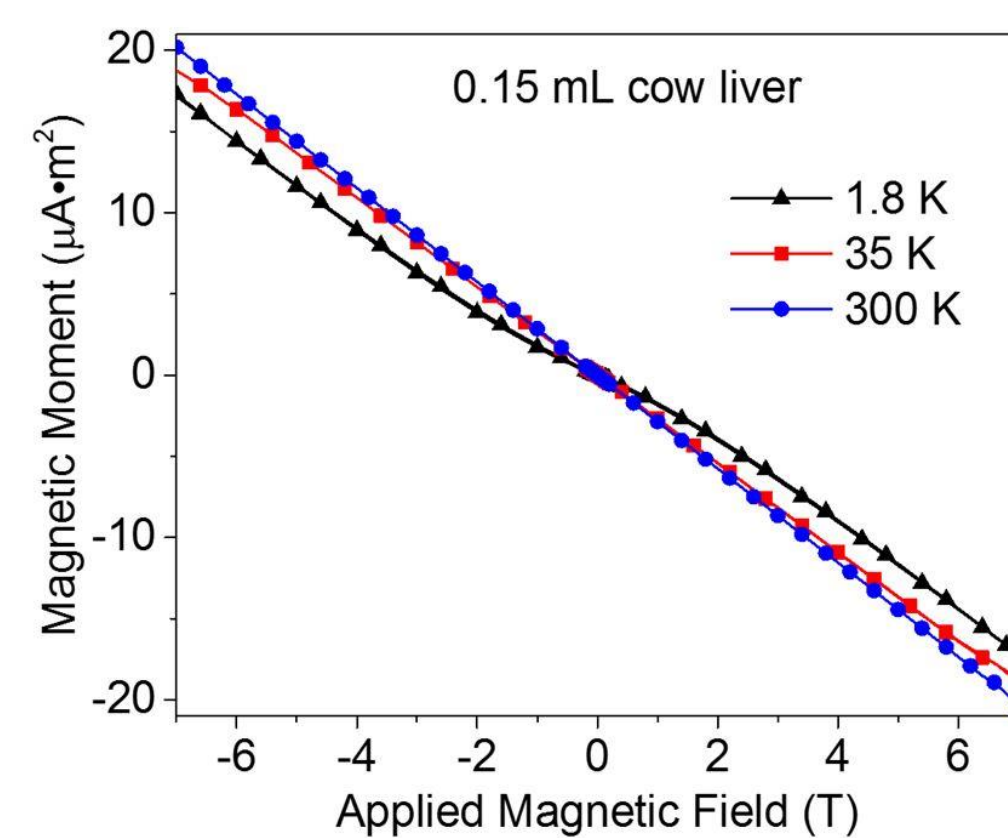
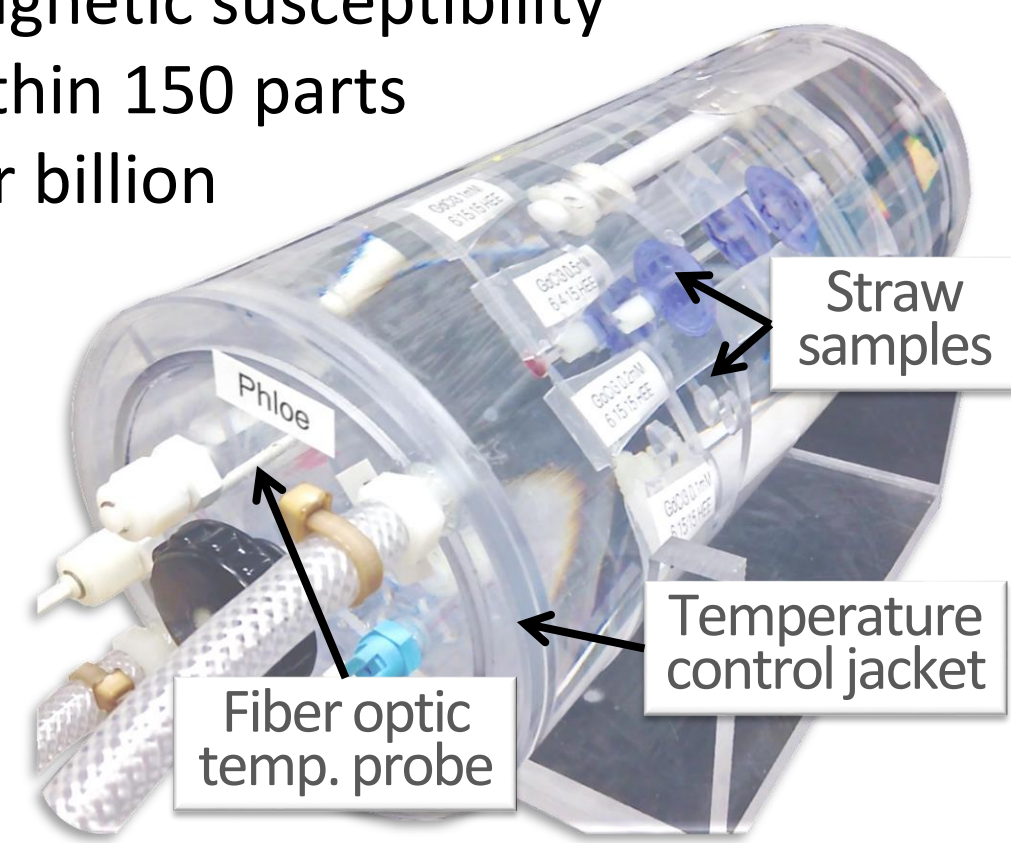
Tan et al. Investigative Radiology 49(7), (2014)

TISSUE SUSCEPTIBILITY & TISSUE MIMICS

Complex magnetic structure of tissue only seen at low temperatures (para/ferri-magnetic components are no longer overshadowed by the diamagnetic component)

Gadolinium chloride solutions provide 1st-order approximation to susceptibility properties of tissue.

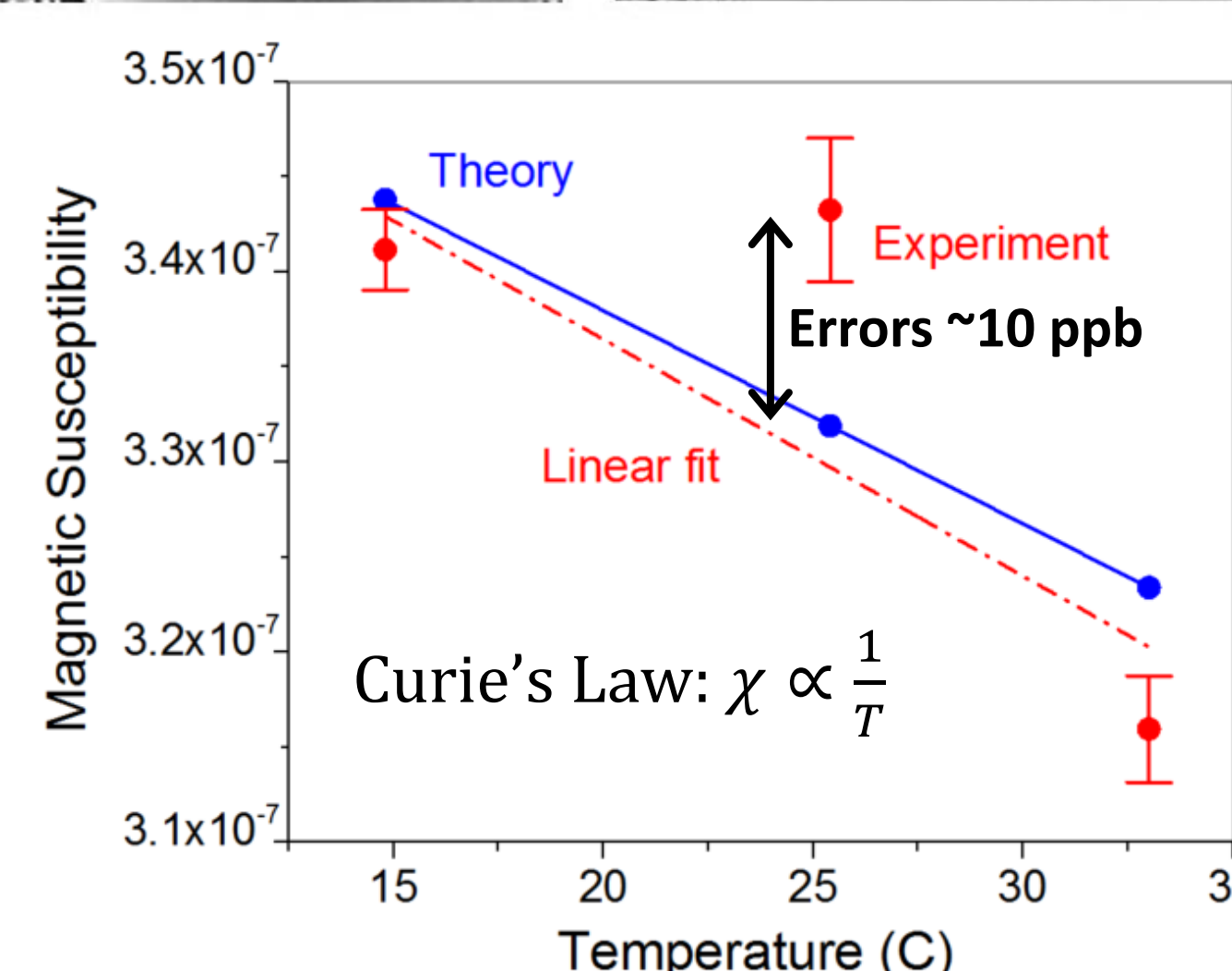
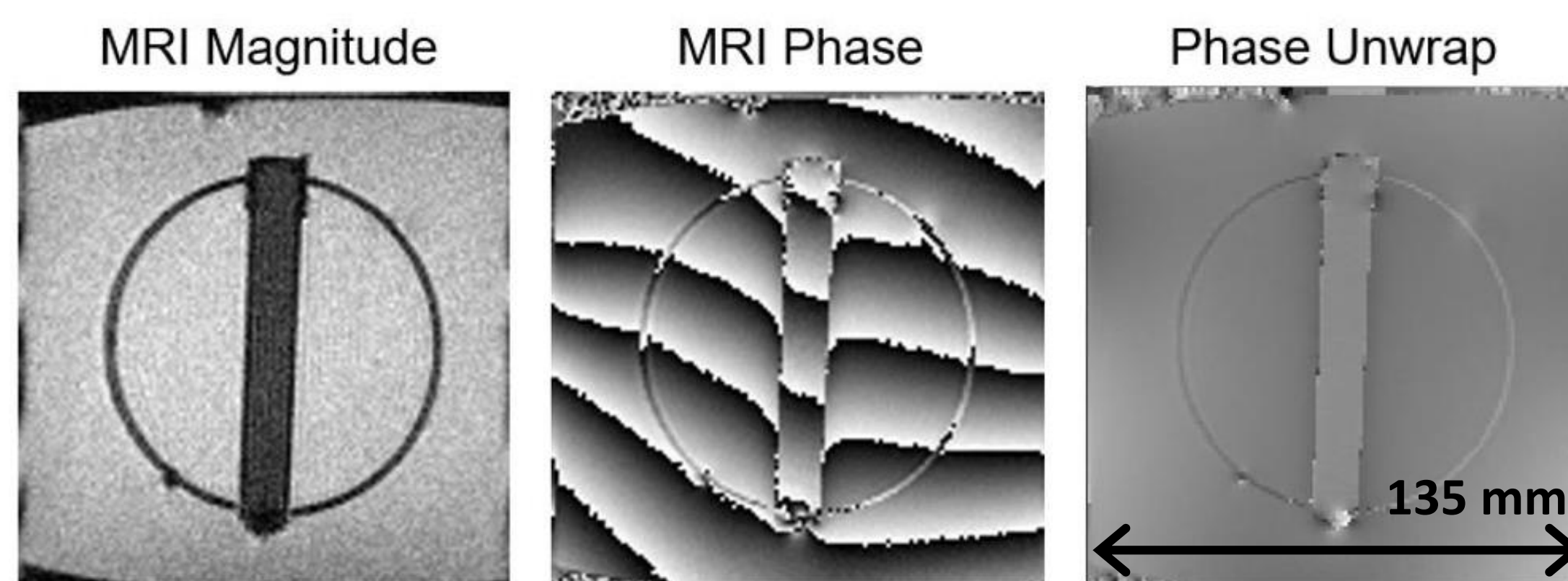
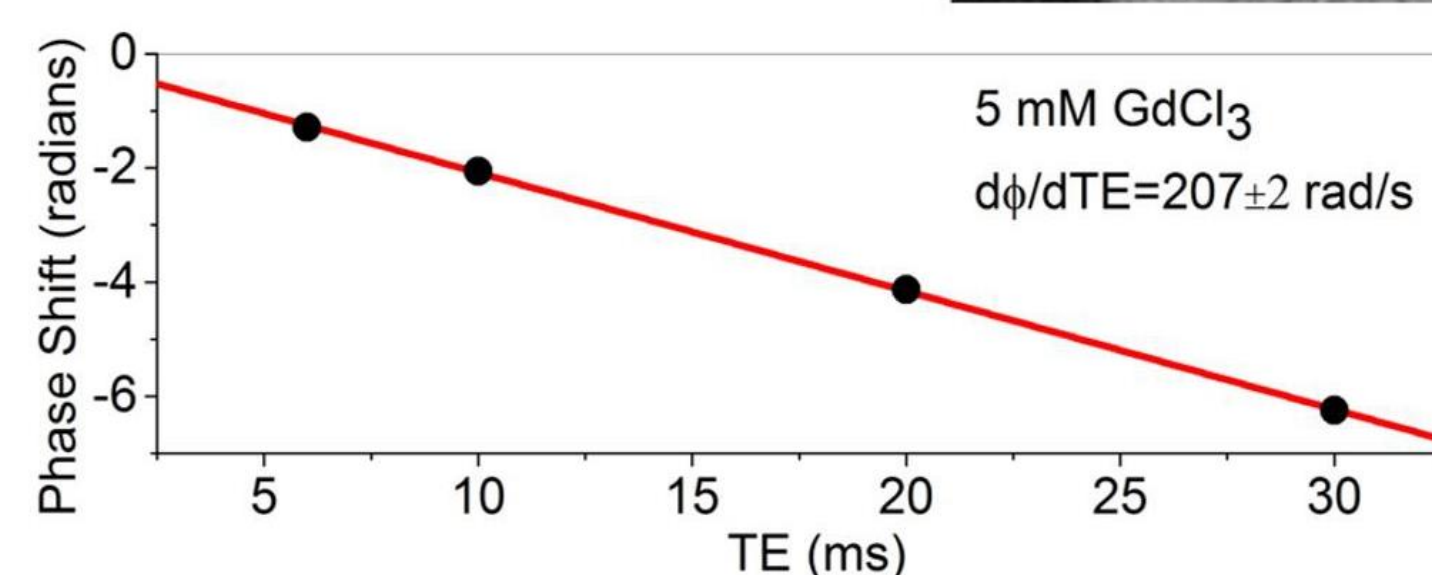
SQUID magnetometer able to measure magnetic susceptibility within 150 parts per billion



MRI SUSCEPTIBILITY MEASUREMENTS

Calibration phantoms were built to scan paramagnetic gadolinium chloride solutions while controlling the temperature or orientation of a cylindrical sample

Scans were made using a gradient echo pulse sequence



Local magnetic fields of a long paramagnetic cylinder, exposed to \mathbf{B}_0 , cause a predictable phase shift proportional to its susceptibility:

$$\chi = \frac{3}{\gamma_p B_0} \cdot \frac{\Delta\phi}{\Delta TE}$$

ANGLE DEPENDENT MEASUREMENTS

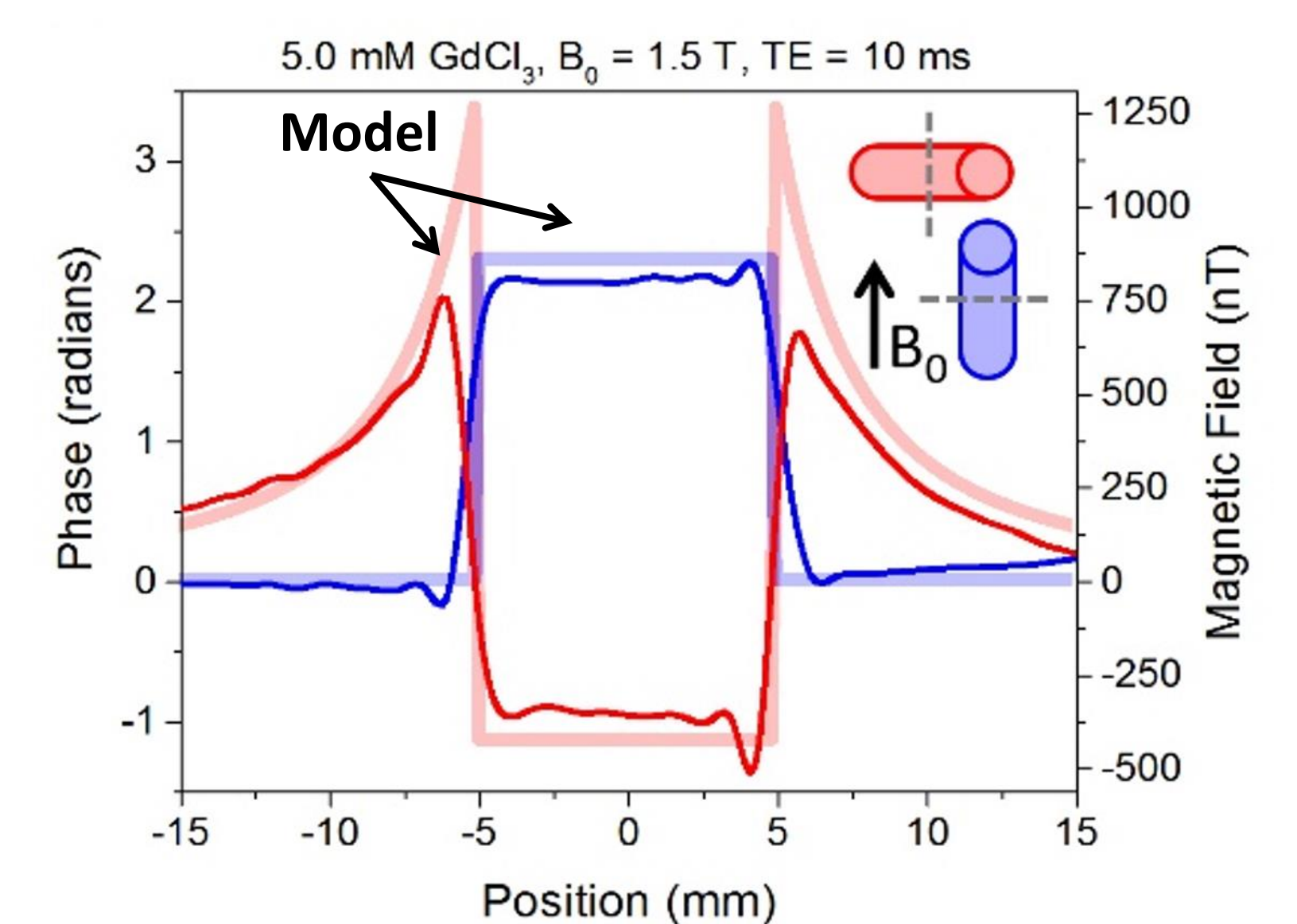
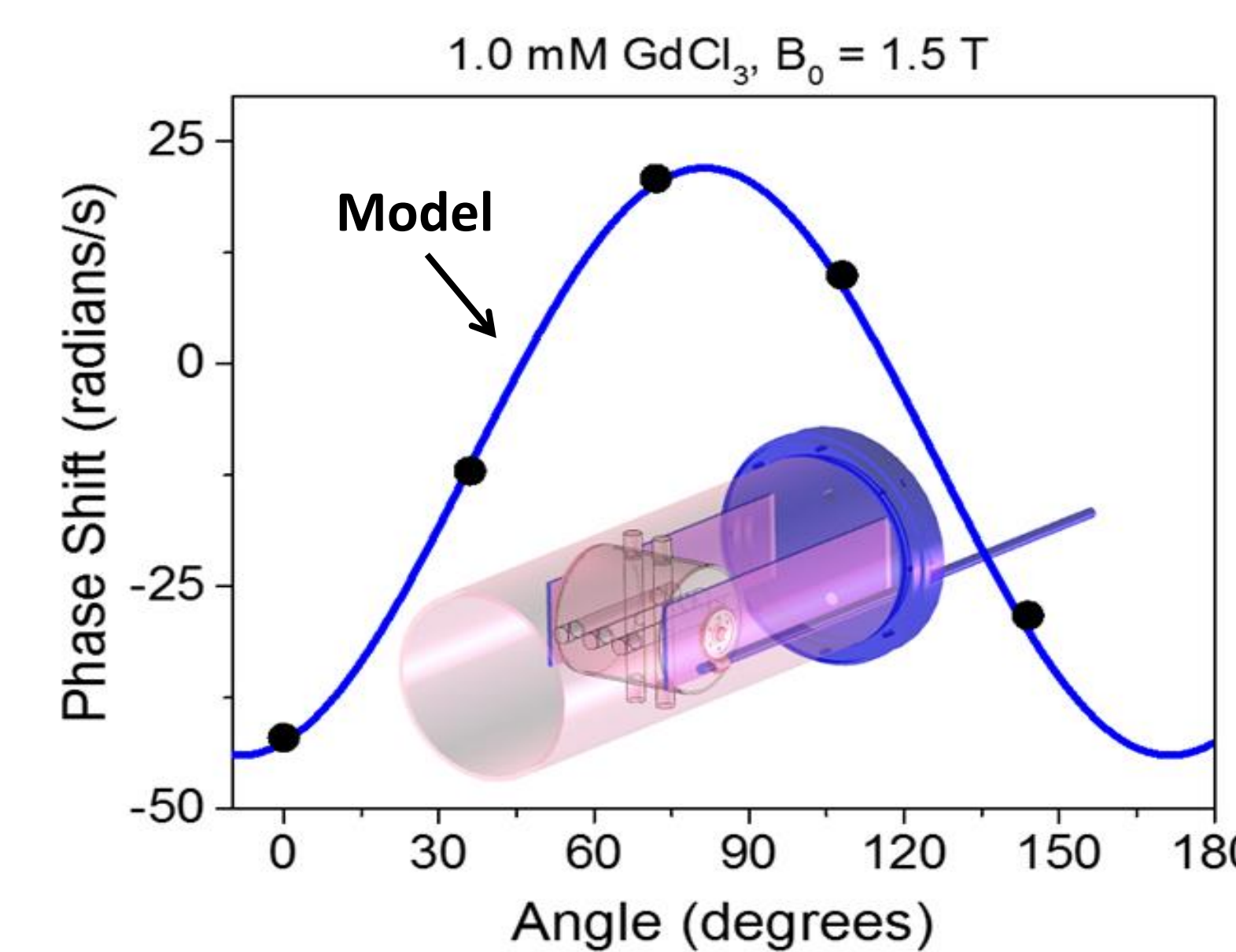
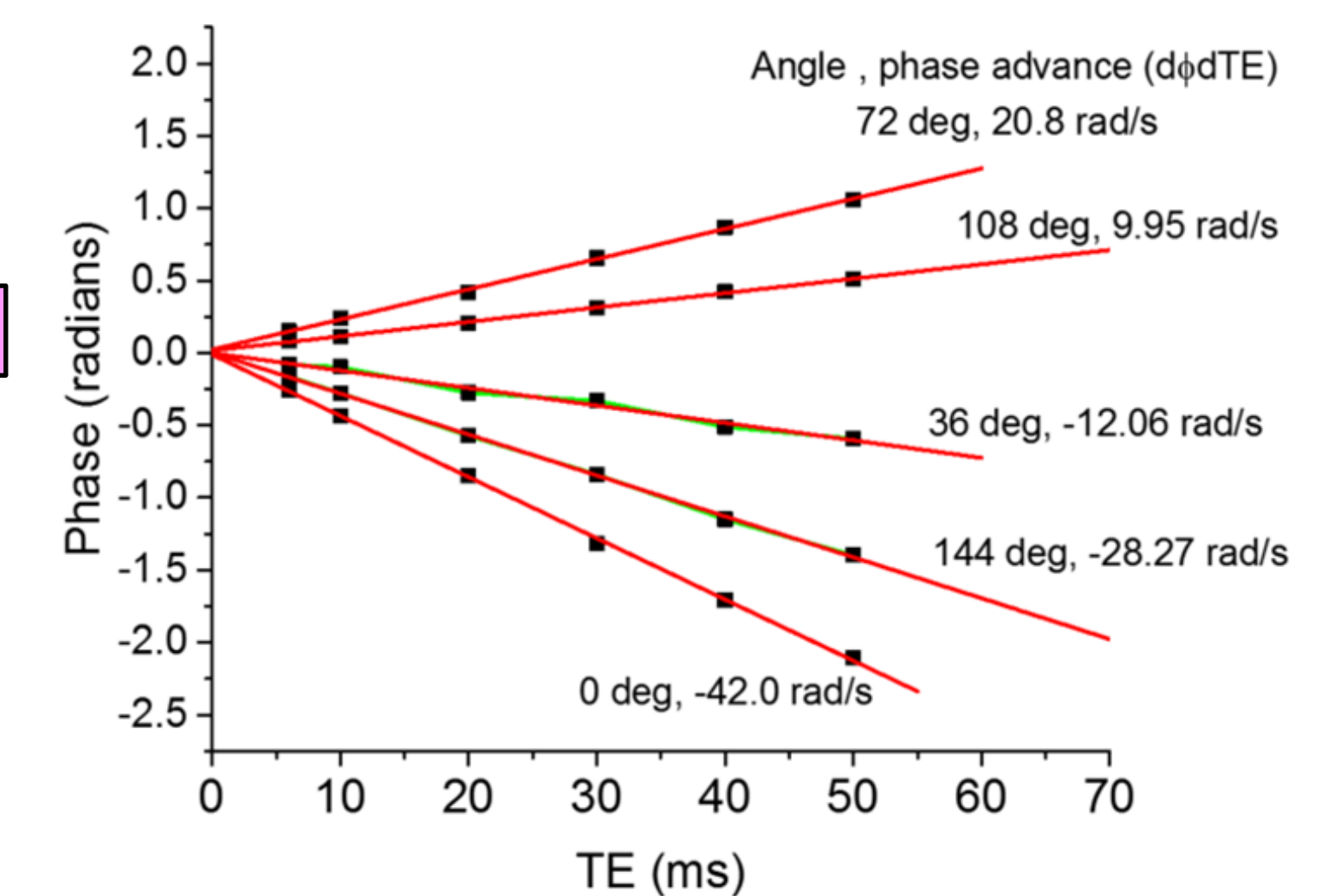
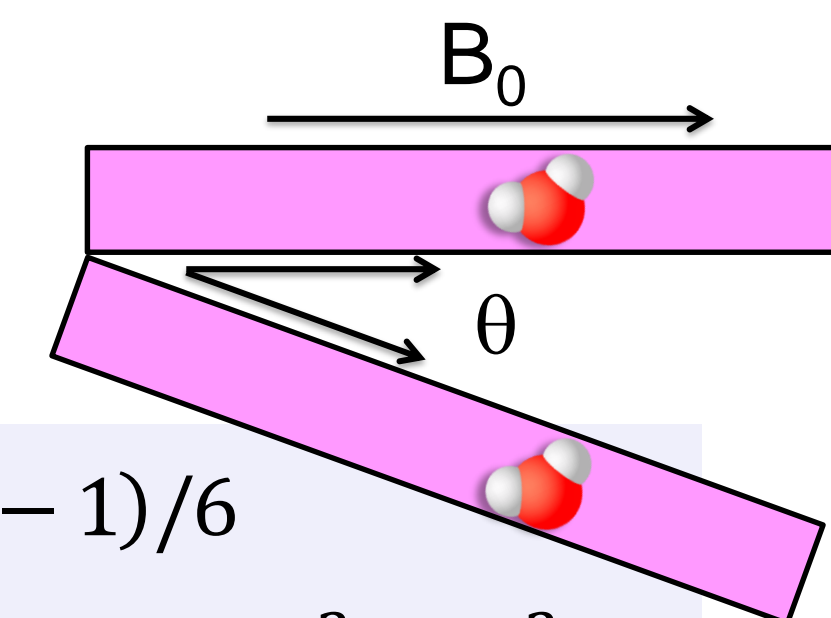
Our measurements closely resembled the predicted shifts in the local magnetic field for a long cylinder with susceptibility $\chi = 1.7 \times 10^{-6}$

Long Cylinder Model:

$$\Delta B_{in} = \Delta\chi B_0 (3 \cos^2 \theta - 1)/6$$

$$\Delta B_{out} = \Delta\chi_{do} B_0 \sin \theta \cos(2\Phi) a^2 / (2r^2)$$

Haacke | AJNR 30 | Jan 2009 | www.ajnr.org



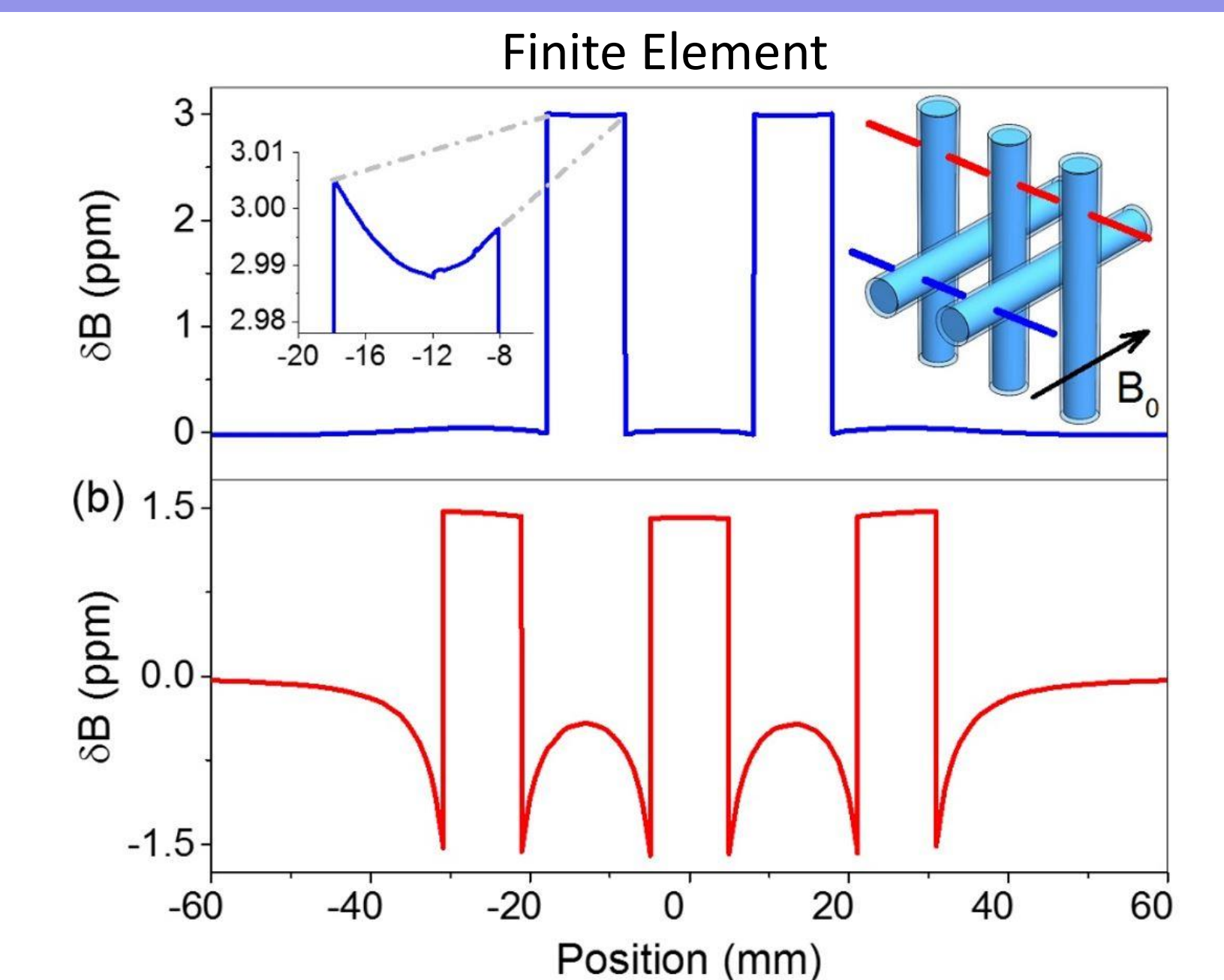
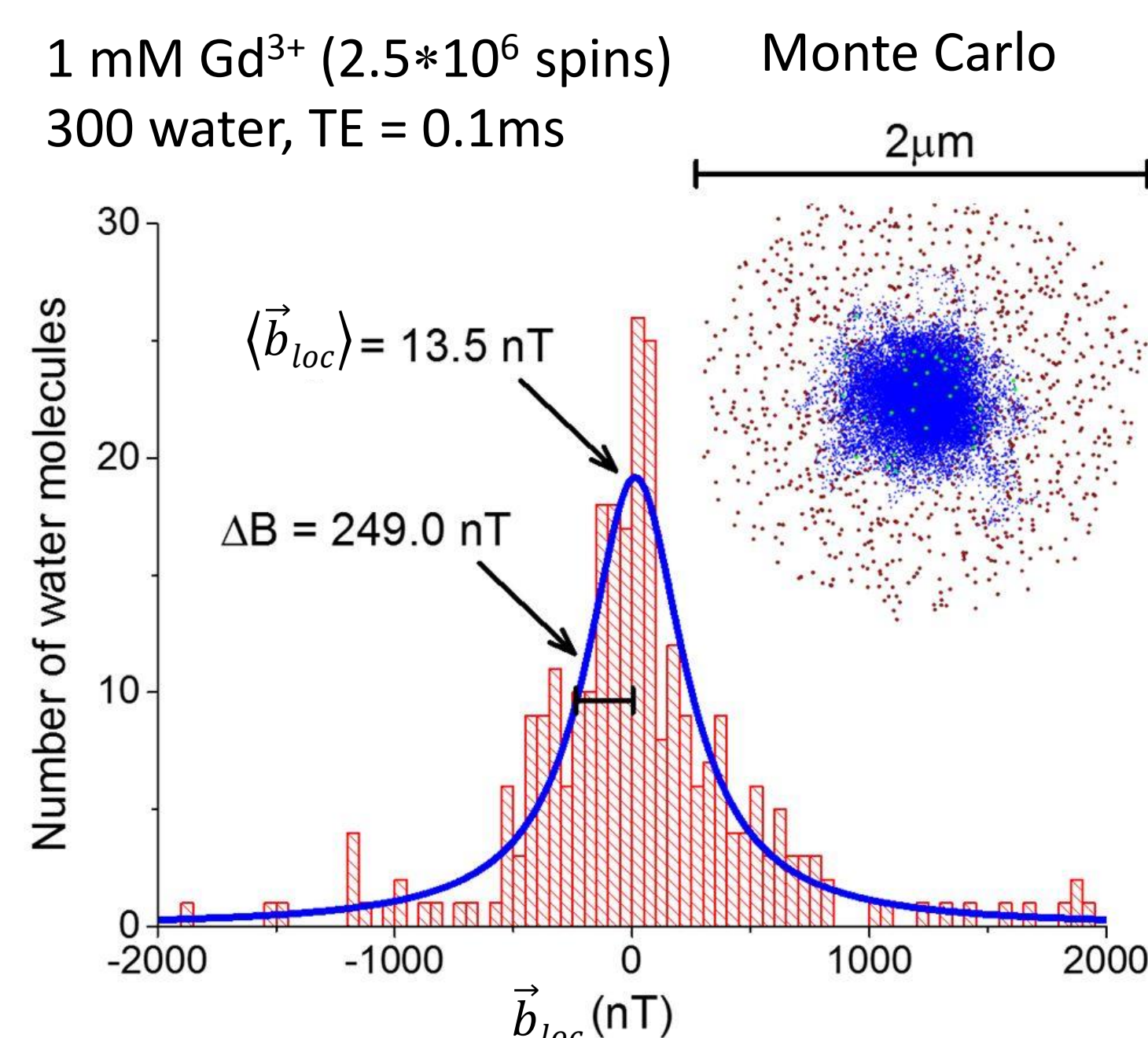
BEYOND THE SIMPLE MODELS

$$\vec{B}_{loc} = \vec{B}_m - \vec{B}_{Lorentz} + \langle \vec{b}_{loc} \rangle$$

Macroscopic field as obtained by FEM

$\frac{2}{3} \mu_0 \vec{M}$

Microscopic field, ave ≈ 0



Finite Element Method simulations were used to determine macroscopic field contribution to \vec{B}_{loc}

Monte Carlo simulations were used to determine microscopic field contribution to \vec{B}_{loc}

Local microscopic field \vec{b}_{loc} distribution and water diffusion determines T_2^*

CONCLUSIONS

Relative resolution of MRI susceptibility techniques is very good (~ 10 ppb), but absolute accuracy is still a problem. SQUID magnetometry (good to ~ 150 ppb) not good enough to develop primary reference material. Conventional ex-vivo tissue magnetometry is less accurate than in-vivo MRI measurements.

Next steps:

- Examine accuracy of susceptibility reconstructed from 3D phase maps (instead of 2D)
- Develop biomimic materials that simultaneously mimic χ , T_1 , and T_2 properties of tissue.
- Understand the field variations of complex tissue at the microscopic level.
- Examine the relationship between susceptibility and blood-oxygen concentration.

REFERENCES

J. F. Schenck, Medical Physics., 23(6): 815-850, (1996) E. M. Haacke, et al, AJNR., 30(1): 19-30, (2009) Haacke and Reichenbach SWI in MRI Wiley Blackwell (2011)
Jain, Varsha. Magn Reson Med., 68(3): 863-867 (2012) Tan et al. Investigative Radiology 49(7), (2014) Elster, A., MD. Questions and Answers in MRI. web. (2015)

Erdevig, et al. AIP Advances 7, 056718 (2017)